



1 **Study on monitoring and numerical analyses of**
2 **groundwater variation and inclinometer displacement**
3 **induced by heavy typhoon rainfall**

4
5 **Ching-Jiang JENG¹, Chia-Yu Yang²**

6 [1]{ Associate Professor, Huaan University, New Taipei City, Taiwan }

7 [2]{ Project Assistant, Huaan University, New Taipei City, Taiwan }

8 Correspondence to: Ching-Jiang JENG (jcjh@cc.hfu.edu.tw)

9
10

11 **Abstract**

12 This study examined the slope area of the Huaan University campus, within the entire Ta-
13 Lun Shan area. Situated at 550 m above sea level, the area is geographically classified as a dip
14 slope. For sustainable development of the campus, a variety of continuous monitoring
15 equipment has been set. This study continues to analyze the monitoring data in the previous
16 period, but focuses on the observation and comparison of the horizontal displacement at
17 different depths recorded by inclinometers with time. At the same time, the relationship
18 between the groundwater variation caused by heavy typhoon rainfall and the driven deep
19 displacement of the slope is studied. In addition, this study has also been extended to the
20 whole Ta-Lun Shan area, the observation data of cracks inside and outside the campus are
21 analyzed. The displacement and sliding data collected over the years by the inclinometers are
22 used to study the potential sliding surfaces distribution of the slope, combined with the
23 influence of the typhoon rainfall. This study also continues to obtain the relationship between
24 groundwater level and rainfall, such as the time lag and groundwater level changes, and
25 reviews the effectiveness of the implementation of two catchpits at the campus. In the process
26 of renovation, a Shape Acceleration Array (SAA) is used for measuring the instantaneous
27 displacement to monitor if the displacement has increased during the implementation of the
28 catchpits. The SAA measurement is taken as the reference basis for hazard prevention and
29 maintenance of the slope, thus reducing and preventing the occurrence of disasters in the area.



1 Then, a series of shear tests are carried out. Finally, the software Geostudio is applied to
2 analyze the relationship between rainfall infiltration, groundwater level, and the displacement
3 of the entire slope. The numerical analysis results are compared with the monitoring results in
4 order to comprehensively discuss the slope safety.

5

6

7 **1 INTRODUCTION**

8 This research focuses on the dip slope area at the Huafan University in northeastern Taiwan.
9 The campus is located on a geological dip slope toward the southwest in the Ta-Lun Shan area
10 with an elevation ranging from 450 to 550 m, as shown in Fig. 1. For risk management and
11 research on slope stability, a monitoring system was set up in 2001, which has collected
12 geographical data since then. The monitoring system includes inclinometers, tiltmeters, crack
13 gages, water-level observation wells, settlement and displacement monitoring marks, rebar
14 strain gages, concrete strain gages, and rain gages.

15 Jeng and Sue (2016) analyzed the monitoring data collected from more than 300 settlement
16 and displacement observation marks on this site and compared them with the displacement
17 recorded by the inclinometers, finding a preliminary relationship between the displacement of
18 the slope and daily rainfall on the campus. The program STABL based on the limit
19 equilibrium method was applied for analysis, concluding that a rise in the groundwater table
20 caused by typhoons is the most critical factor in slope stability. Therefore, several
21 countermeasures, including catchpits with horizontal drainage pipes, were recommended, and
22 threshold-value curves of the slope displacement based on rainfall intensity and cumulative
23 rainfall were established. Those curves were derived from the rainfall records of numerous
24 typhoon events over the past ten years, along with the corresponding slope displacement
25 increment recorded by the ground surface marks.

26 The Japan Association for Slope Disaster Management (JASDiM) recommended the threshold
27 values of slope displacement for different sliding stages, which were used to define three
28 ranges. However, the displacement data recorded by the inclinometers used in the study were
29 retrieved once a month, and the displacement and subsidence of the slope by the observation
30 points were observed every six months. Therefore, the instantaneous changes of each typhoon
31 rainstorm event could not be known. An additional groundwater level gauge was installed in
32 the study area, and two Shape Acceleration Arrays (SAA) were installed within the



1 inclinometer casings, which have observed depths of sliding surfaces. This has made it
2 possible to obtain the continuous changes of groundwater level and slope displacement during
3 typhoon rainfall. Slope stability was also analyzed during the period.

4 Considering the project budget, two catchpits were implemented within the study area in the
5 present stage. The study provides valuable monitoring information and experience as
6 continuation of campus observations for years. The study also offers a comprehensive survey
7 of the slope behavior during rainfall infiltration, including the highest groundwater level
8 measured within the slope, the time lag reaction of groundwater variations, the influence of
9 rainfall types and amount, the relationship curve of rainfall amount and groundwater level,
10 and a review of the effectiveness of the two catchpits. The displacement curve measured by
11 the inclinometers was used for feedback comparison, and numerical analysis and simulation
12 were performed to validate the changes in the behavior and mechanism. Then, according to
13 the characteristics of the slope, including the allowable displacement alert and action values,
14 the data analyses revealed a corresponding relationship rainfall curve. The results will help
15 assess possible changes in groundwater level within the slope, possible slope displacement,
16 and safety and stability factors from the estimated rainfall before a disaster occurs.

17 Generally, slope displacement can be distinguished into several stages, in which the three
18 stages are: “initial displacement,” “constant velocity displacement,” and “accelerated
19 increment displacement.” Xu (2011) pointed out obvious stages characteristics for the gradual
20 evolution of slope variations. To classify a type of displacement into one of the three stages,
21 the s-t curve for the relationship between displacement and time can be converted into a T-t
22 curve. The curve after conversion has a unique and deterministic tangent angle (α). Normally,
23 the tangent angle of the curve is greater than 45 degrees when it enters the acceleration stage.
24 Detailed demonstration of each deformation stage is shown in Figs. 1(a) and (b).

25 **2 SITE INFORMATION**

26 The Huafan University is located on a hillslope. Over the years, with the support of the
27 university and the Ministry of Science and Technology, more than 40 inclinometers (Fig. 2),
28 two surface extensometers, 48 rebar drain gauges, 36 concrete strain gauges, and 28 tiltmeters
29 have been installed at the campus. In addition, more than 300 ground subsidence and
30 displacement observation points with ground surface and structural crack detection records.
31 All of these monitoring instruments are continuously operational in taking regular
32 measurements. This combination of a wide range of experimental site information is a



1 valuable repository of data for both national and international research. With the joint efforts
2 of various authors in the past years, this site has focused on the monitoring system, geological
3 and hydrological data, and the establishment of a geographic information system, generating a
4 significant amount of research results (see Chao, 2002, 2003; Jeng, 2003, 2007; Jeng and Sue,
5 2009, 2016; Jeng and Lin, 2011, 2014; Jeng and Jiang, 2013; Jeng et al., 2015, 2017).

6 The main exposed stratum under the site is the Mushan Formation, with the bedrock being
7 mainly interbedded with sandstone and shale. It is a dip slope striking toward the east, dipping
8 southward about 10°–20°. Huang and Jeng (2004) pointed out that through the observation
9 and comparison of drilling cores and ground resistance images, as well as topographical
10 characteristics, there are two local small faults: a south-trending Nanshihkeng Fault and a
11 northwest-trending A Fault, as shown in Figure 3.

12 In addition to the above monitoring system, surface crack observation within the site is
13 conducted every six months. Cumulative observation results show continuous growth of the
14 number and size of the surface cracks over time. Therefore, continuous renovation and
15 reinforcement works have been carried out for the past few years. Figure 4 is the location map
16 of the surface cracks inside and outside the campus.

17 **3 STUDY RESULTS AND DISCUSSIONS**

18 **3.1 Analyses of monitoring results of auto-recording groundwater level gauges**

19 According to the basic information of the research site and the inclinometers, tiltmeters,
20 groundwater level gauges, building inclination measurements, displacement and subsidence
21 observation points, surface crack investigation and other monitoring equipment system data,
22 as well as the geological and hydrological data, analyses of the automatic groundwater level
23 monitoring results at the campus are as follows.

24 Analyses of historical data show that rainfall causes the slope displacement. In order to
25 understand the relationship between rainfall and the groundwater variation and the slope
26 stability, four sets of auto-recording groundwater-level gauges are designed in this research
27 area for observation and discussion. The configuration diagram of the groundwater -level
28 gauge (piezometer) is shown in Fig. 2. Additionally, Fig. 5 through Fig. 8 illustrate some of
29 the monthly rainfall data and groundwater-level changes from 2013 to 2016.

30 Figure 5 is a diagram of rainfall data and groundwater-level duration curves in April 2013.
31 The x-axis is the time, the left y-axis is the groundwater level (expressed as depth below GL),
32 and the right y-axis is the rainfall. The groundwater level in W1 has a dark blue curve, the



1 groundwater level in W2 has a red curve, the groundwater level in W3 has a green curve, and
2 the groundwater level in W4 has a purple curve. The light blue curve is the rainfall in April.
3 Figure 5 indicates that three heavy rainfalls occurred in April, on 4/1–4/5, 4/8–4/13, and
4 4/17–4/20. Their rainfall types can be classified as post-peak rainfall, pre-peak rainfall, and
5 pre-peak rainfall, respectively. Additionally, when rainfall occurs, groundwater level also
6 changes, although with some time lag. The degree of groundwater level change is
7 $W1 > W2 > W3 > W4$, which indicates that degree of change of the groundwater level in
8 observation wells is different across different regions.

9 The monitoring data from Fig. 6 to Fig. 8 of the rainy and typhoon seasons in 2015–2016 was
10 analyzed using the same method. Similarly, the W1 groundwater level change is particularly
11 evident, with the groundwater level change uplifted by rainfall up to about 23 m, while in W2,
12 W3, and W4, the amount of change was about 8 m, 6 m, and 1 m, respectively. This indicates
13 that the groundwater level in the area of W1 was more susceptible to rainfall influence. If
14 heavy rainfall happens in the future, the area near W1 must be closely monitored. A
15 comparison of different rainfalls shows that the peak rainfall of post-peak rainfall was greater
16 than the peak of other types of rainfall, so post-peak rainfall should be monitored more
17 closely. Furthermore, in Fig. 5, it is shown that during the rainy season in April, the rainfall
18 period is short, and the rainfall amount is mostly less than 40 mm; the groundwater level rise
19 speed is slow, and the rising amount is small. Figures 6–8 report the rainfall data from the
20 typhoon season, from August to October, during which the rainfall is mostly greater than 40
21 mm. Additionally, during the typhoon season, rainfall will cause greater rise of the
22 groundwater level, and the lag time between the peak rainfall and peak groundwater level will
23 significantly shorten. When the groundwater level in W1 rises to about ground level (GL) -30
24 m, W2 and W3 will then increase more noticeably. Based on the above information, during
25 the typhoon season, W1 can be used as an important observation index for alerts and
26 protective measures to avoid problems with the slope stability change.

27 Given the above analyses, it is clear that groundwater-level change caused by rainfall can vary
28 due to (1) rainfall type, (2) rainfall amount, (3) rainfall time lag, (4) groundwater-level gauge
29 region, and (5) seasonal factors. Analyses of these factors are illustrated in Figs. 9–11, which
30 contain only analysis data from observation well W1. These figures are, in this order, the
31 groundwater level and rainfall peak time lag diagram, the peak rainfall and groundwater-level
32 rise diagram, and the accumulated rainfall and groundwater-level rise diagram for W1



1 groundwater-level gauge from 2013 to 2015.

2 Figure 9 is the groundwater level and rainfall peak time lag diagram of automatic
3 groundwater-level gauge W1. The x-axis is the peak rainfall, and the y-axis is the time lag for
4 groundwater level to reach its peak. Figure 10 is the peak rainfall and groundwater level rise
5 diagram of automatic groundwater-level gauge W1. The x-axis is the peak rainfall, and the y-
6 axis is the amount of groundwater level rise. Figure 11 is the accumulated rainfall and
7 groundwater-level rise diagram of automatic groundwater-level gauge W1. The x-axis is the
8 accumulated rainfall, and the y-axis is the groundwater-level rise amount. The round dots are
9 post-peak rainfalls, the square dots are pre-peak rainfalls, and the triangle dots are middle-
10 peak rainfalls. There are two types of accumulated rainfall: accumulated up to the peak (dark-
11 colored symbols) and accumulated for the entire rainfall (light-colored symbols).

12 Figure 9 shows that the greater the peak rainfall, the shorter the reaction time lag is for the
13 groundwater level to rise. With respect to the rainfall type perspective, the peak rainfall of the
14 pre-peak rainfalls is concentrated less than 20 mm and has a long groundwater-level time lag.
15 The peak rainfall of the middle-peak rainfalls ranges from 20 mm to 40 mm, and the peak
16 rainfall of the post-peak rainfalls is concentrated at around 50 mm with a short time lag. It
17 indicates that if this study area has rainfall greater than 50 mm, it should be closely observed
18 and the observation time should be stretched to about 40 hours. Further, Fig. 10 shows that for
19 greater peak rainfall, the groundwater level will significantly increase, and the post-peak
20 rainfall will cause the most significant groundwater level rise. According to the auto-
21 recording groundwater-level gauge, the groundwater rise amount was between 1 and 23 m.
22 Lastly, Fig. 11 shows that when the total average cumulative rainfall to peak point exceeds
23 200 mm, the groundwater level in auto-recording groundwater-level gauge in W1 will
24 increase up to 20–23 m.

25 W2–W4 were observed and analyzed by using the same method, and the results indicate that
26 if the rainfall type is the post-peak, the time lag for its groundwater level to reach the peak is
27 the shortest, resulting in the largest increase in its groundwater level. Moreover, when average
28 cumulative rainfall exceeds 200 m, significant groundwater-level increase will occur,
29 requiring close observation for up to 40 hours.

30 As mentioned above, when the peak rainfall is greater, the time lag of the groundwater level
31 rise will be shorter. The peak rainfall of the post-peak rainfall type is greater than that of other
32 rainfall types, which makes the change of its groundwater level significant. Thus, observation



1 for up to 40 hours is needed for the post-peak rainfall. The data from the auto-recording
2 groundwater-level gauge shows that the groundwater level W1 is most affected by rainfall,
3 with a change between 1 m and 23 m. A groundwater-level change of 0.6–5.8 m was found in
4 the auto-recording groundwater-level gauge in W2, 0.25–3.1 m in W3, and 0.1–2 m in W4.

5 **3.2 Analysis and discussion of inclinometer displacement**

6 The location of the inclinometers at the site is shown in Fig. 2. This study used
7 cumulative rainfall amount from previous typhoon alerts and the displacement of 29
8 inclinometers to observe the displacement of the inclinometer casings and aggregated the data
9 into graphs to show the trend. The data are organized sequentially based on the gradual
10 evolution of slope change over time as recorded in previous research. The present study only
11 used nine casings with a relatively large displacement and only the analysis of inclinometer
12 SIS-32 was used as an example, as shown in Fig. 12:

13 Figure 12 is the SIS-32 displacement and cumulative rainfall amount from typhoon rainfall.
14 The x-axis is the cumulative rainfall amount from typhoon rainfall, and the y-axis is the
15 displacement caused. Different inclinometer displacements from different typhoons in the
16 past years are presented in the graph. The data curve pattern was classified as gradual change
17 type referring to the damage curves pattern classification presented by Xu (2011) shown in
18 Fig. 1. The graduated pattern means that the displacement will be different (for different
19 rainfall amount) at different times, and the change will accelerate when a certain rainfall
20 amount is reached. Once the displacement starts to accelerate, the accumulated rainfall is
21 treated as an alert rainfall threshold value. Figure 12 shows the typhoon cumulative rainfall
22 alert of SIS-32 has a threshold of about 350 mm.

23 The typhoon cumulative rainfall alert threshold values from the other nine inclinometers are
24 summarized in Table 1, and positions of the inclinometers with accelerated displacement
25 history are plotted on the map in Fig. 13. Table 1 shows that the alert cumulative rainfall
26 threshold for heavy typhoon rainfall causing campus slope displacement is approximately
27 315–495 mm. The threshold is relatively low in the Sport ground and near Wu-Ming Building,
28 meaning that it has a higher degree of hazardous urgency. Figure 13 shows that the available
29 data thus far show that regions at the campus where heavy typhoon rainfalls reached alert
30 threshold value are: (1) the area surrounded by Wu-Ming Building, Hui-Tsui Building, and
31 the Library Building; (2) from the Sport ground to the slope of Material laboratory; and (3)
32 from Lotus garden outside the campus to Ta-Lun road. Therefore, these three regions should



1 be the focus of slope safety maintenance and future monitoring of slope displacement during
2 typhoon rainfall.

3 The campus already has existing groundwater monitoring data, as previously discussed, to
4 understand the lifting and possible flow of the groundwater at slope above the A Fault.
5 However, the campus slope has experienced large displacement during the rainy season when
6 the groundwater level is high. Considering the above data analyses, it is recommended that
7 the Wu-Ming Building at the campus should be accorded priority consideration in future
8 heavy rainfall events for safety improvement needs. Accordingly, two catchpits were
9 implemented below and above the Wu-Ming Building slope (Fig. 2) to reduce or adjust the
10 groundwater level for enhanced slope safety and stability.

11 **3.3 Maximum groundwater level monitoring data and analysis to explore the** 12 **effectiveness of catchpits**

13 In this study, simple groundwater level gauges were mounted to manually obtain the highest
14 groundwater-level readings for observations and discussions. The six highest groundwater-
15 level gauges were mounted to inclinometers SIS-1, SIS-9, SIS-11, SIS-26, SIS-32, and SIS-38,
16 as shown in Fig. 2. The highest groundwater-level-variation data from some of the
17 inclinometers from April to July 2016 are plotted in Figs. 14–15.

18 Figure 14 is the relation graph of rainfall data and groundwater level from the auto-recording
19 groundwater-level gauge from April to July 2016. The x-axis is time, the left y-axis is the
20 water level, and the right y-axis is the rainfall amount of the day. The groundwater level from
21 the auto-recording groundwater-level gauge in W1 has a red curve, the water level in W2 has
22 a green curve, the water level in W3 has a purple curve, and the groundwater level in W4 has
23 a light blue curve. The dark-blue curve shows the daily rainfall amount from April to July.
24 The figure shows that, similar to aforementioned data, W1 is much more affected by the
25 rainfall amount than the other three auto-recording groundwater-level gauges. The data from
26 the auto-recording groundwater-level gauge in W1 from 2013 to 2016, as shown in Fig. 15,
27 shows that the normal groundwater level from the auto-recording groundwater-level gauge in
28 W1 has a lowest value of about -43.67 m from 2013 to 2015. After the implementation of the
29 catchpits in 2016, the lowest curve has decreased significantly to -52.03 m. The highest
30 groundwater level also dropped from -22.67 m to -27.84 m. This is due to the
31 implementation of the two catchpits at the site, which significantly reduced both normal
32 groundwater level and the highest groundwater level during rainy and typhoon seasons.



1 Figure 16 is the groundwater level rise amount distribution from the aforementioned six
2 highest groundwater-level gauges. It is clear from the figure that the groundwater level
3 variation in the region between the A Fault and the Nanshihkeng Fault is very large (mostly
4 higher than 21m as shown in Fig. 16), while the groundwater-level variation in the region
5 below the Nanshihkeng Fault is relatively small. The current findings thus conclude that SIS-
6 32 located out of the area enclosed by the Nanshihkeng Fault and the A Fault, enabling the
7 groundwater from rainfall infiltration to smoothly flow down the slope, so the groundwater-
8 level rise (6-8m) is less than the region surrounded by the two faults.

9 **3.4 Discussion of SAA displacement measurement results**

10 The current manual measurement of the inclinometers occurs at the frequency of once a
11 month. The drawback is that it is unable to measure the correct amount of displacement
12 caused by heavy typhoon rainfalls and that there are errors caused by manual measurements.
13 In order to improve the situation, the SAAs have been implemented since 2014 at 3 m long
14 above and below the sliding depth at the inclinometers SIS-11 and SIS-20 in the vicinity of
15 Wu-Ming Building (Fig. 13). The SAA sensors are implemented every 0.5 m, with total 12
16 sensors setting in each inclinometer. Starting from 2017, two new SAAs are added for SIS-1
17 and SIS-8. In addition to the benefits of its continuity (one measurement every 10 min), high
18 precision, wide range of deformation measurement and automatic readings to compensate for
19 the drawbacks of manual reading of inclinometers, another purpose for the use of SAA is to
20 monitor if excessive slope displacement occurs before and after the implementation of
21 catchpits, in order to better fulfill the purpose of the warning system.

22 This study used rainfall data and SAA displacement from April 2014 to November 2017 to
23 observe and analyze the relationship between them. Data were aggregated to show trends,
24 such as in Fig. 17, which contain data captured and amplified from June 2014 as examples.

25 Figure 17 is respectively the relationship between inclinometer displacement of SIS-11 and
26 SIS-20 and rainfall amount from June 2014. The x-axis is the date, the left y-axis is the daily
27 rainfall amount, and the right y-axis is the daily accumulated displacement of inclinometers
28 SIS-11 and SIS-20. On June 19 and 23, 2014, there were heavy rainfall (hourly rainfall
29 amount > 100 mm), and the displacement also rapidly increased due to two continuous heavy
30 rainfall, demonstrating that displacement increases with rainfall amount, and continuous
31 heavy rainfall will make the slope displacement even more evident.

32 The above analyses show that the displacement varies due to the following factors: (1) rainfall



1 amount, (2) continuous heavy rainfall, and (3) environmental conditions at the inclinometer
2 position. The cumulative rainfall and SAA displacement increment information is
3 summarized in Table 2, which shows the obtained cumulative rainfall amount and the
4 increment of the cumulated displacement amount.

5 Using the data in Table 2, the minimum driven displacement of daily rainfall turns out to be
6 77 mm/day; if it is less than 77 mm/day then it belongs to steady state. The other point worth
7 noting is that the data obtained from Table 2 are much less than the comprehensive results
8 over the years (Jeng and Sue, 2016). This is because since the implementation of SAA until
9 November 2014, no heavy typhoon rainfalls took place during monitoring. Thus, Table 2 is a
10 general reference for ordinary heavy rainfall. The analysis below concerns situations relevant
11 to typhoon rainfall.

12 This study sought to understand slope displacement caused by typhoon rainfall, so the
13 collection of rainfall data and SAA displacement data continued until February 2017 to
14 observe and analyze the relationship between typhoon rainfall and displacement of SAA. The
15 results are aggregated into charts to observe trends, as shown in Fig. 18 and Fig. 19.

16 Figures 18 and 19 are respectively the relationship graph between the displacement of
17 inclinometer SIS-11 and inclinometer SIS-20 and the rainfall amount. The x-axis is the month,
18 the left y-axis is the rainfall amount, and the right y-axis shows the accumulated displacement
19 of inclinometer SIS-11 and inclinometer SIS-20. These figures show a significant increasing
20 trend of displacement during July–September 2015 and September–October 2016, and the
21 displacement of SIS-11 is slightly larger than the displacement of SIS-20. In this paper, only
22 part of the data was taken and enlarged, shown in Figs. 20–21. The x-axis is the date, the left
23 y-axis is the rainfall amount, and the right y-axis shows the accumulated displacement of
24 inclinometer SIS-11 and inclinometer SIS-20.

25 As shown Figures 20 to 21, there were two typhoons in August 2015, the medium typhoon
26 Soudelor and the strong typhoon Goni. Accordingly, SIS-11 had displacement of 6.048 mm
27 and 1.489 mm, respectively, and the displacement of SIS-20 was 4.839 mm and 1.64 mm,
28 respectively. In October 2016, there was light typhoon Aere along with its peripheral
29 circulation. SIS-11 had a consequent displacement of 11.321 mm, while SIS-20 had a
30 displacement of 3.384 mm. The above data are plotted in Fig. 22 as an SAA displacement
31 increment graph during typhoon rainfall.

32 Figure 22 shows that when the typhoon cumulative rainfall reaches 184 mm, significant



1 displacement will occur; when the cumulative rainfall reaches 300 mm or more, or when the
2 peak rainfall exceeds 156 mm, the displacement will begin to accelerate, producing
3 displacement larger than 3 mm. This result agrees with that in Section 3.2 of this study.
4 Therefore, the study sets typhoon rainfall of more than 300 mm as the alert threshold. In other
5 words, if the weather forecast reports a typhoon rainfall of more than 300 mm, then the
6 displacement situation should be closely monitored.

7 When considering the ordinary typhoon situation, the daily cumulative rainfall and SAA
8 displacement increment relation diagram can be extended to February 2017. The result shows
9 that a daily cumulative rainfall of up to 300 mm the displacement will accelerate. In a typical
10 typhoon situation, the average formula can be used to deduce the displacement increments.
11 The results are plotted in Table 3 for future reference.

12 **3.5 Discussion of Geostudio simulation results**

13 In this study, the aforementioned geological and hydrological data of the site were entered
14 into GeoStudio software to carry out SEEP/W, SLOPE/W, and SIGMA/W numerical analysis.
15 The simulation results were compared to the monitoring data to analyze the effect of rainfall
16 on the slope.

17 **3.5.1 SEEP/W analytical results**

18 This study analyzed the initial condition setting: boundary conditions of rainfall infiltration
19 are shown in Fig. 23, wherein AB is a boundary of the lower constant head slope, and the
20 total head height is set to $H = 387.8$ m; CD is the head boundary of the upper slope, and the
21 total head height is set to $H = 534.5$ m. The upper and lower boundaries of the head setting
22 mainly use the average groundwater level from historical monitoring data. The BC is the
23 impervious boundary ($Q = 0$); AD is the boundary of rainfall infiltration. Table 4 shows the
24 input parameter for the analysis, Fig. 24 is the soil groundwater characteristic curve, and Fig.
25 25 shows the input value of hydraulic conductivity curve, which is mainly based on the
26 resulting of colluvium soil test in pressure plate. These two parameters form a function of
27 groundwater characteristic curve (Fig. 24), and then the groundwater characteristic curve is
28 converted into hydraulic conductivity curve (Fig. 25).

29 This study used rainfall data during typhoons in August 2015 and October 2016, the amount
30 of groundwater-level variations from four auto-recording water-level gauges, as well as two
31 auto-recording inclinometer SAAs, to observe and analyze the relationship between rainfall
32 amount during typhoon, slope displacement, and groundwater-level variation. The results are



1 aggregated to show the trend. The groundwater level data and the automatic inclinometer
2 SAA data were taken from the Huafan University slope center. The rainfall data were taken
3 from the weather station at the Huafan University.

4 Figures 20 and 21 show that two typhoons struck in August 2015, the typhoon Soudelor
5 during 8/6–8/9, and the typhoon Goni during 8/20–8/23. Soudelor generated a rainfall amount
6 of 342.5 mm, an SIS-11A displacement increment of 6.048 mm, and an SIS-20A
7 displacement increment of 4.893 mm. Typhoon Goni generated a rainfall amount of 30.5 mm,
8 an SIS-11A displacement increment of 1.489 mm, and an SIS-20A displacement increment of
9 1.64 mm. A southern low-pressure system (typhoon Aere) generated a rainfall amount of 794
10 mm, an SIS-11A displacement increment of 11.321 mm, and an SIS-20A displacement
11 increment of 3.384 mm. The rainfall amount and actual displacement data were used as a
12 reference in the GeoStudio software simulation analysis.

13 The groundwater-level simulation results from Figs. 26–28 demonstrate that groundwater
14 level will increase during typhoon. The groundwater level variation is 0.6–1.65 m during the
15 typhoon Soudelor, 0.09–1.16 m during the typhoon Goni, and 0.01–5 m during the southern
16 low-pressure system (Aere typhoon). This indicates that different typhoon rainfall amount
17 caused different groundwater-level variations: the greater the typhoon rainfall amount is, the
18 greater the groundwater-level varies, but the degree of groundwater level variations is smaller
19 than the actual monitoring data (average 18 m). The possible factors are (1) the hydraulic
20 conductivity of the simulated soil, (2) infiltration reduction coefficient, (3) the water head of
21 slope, (4) element mesh size, (5) normal rainfall amount in steady state, (6) actual position of
22 cross-sectional soil model, and (7) boundary conditions of cross-sectional variations and the
23 parameter settings. Since most of the parameters of this study were hypothetical, there is a
24 certain distance from the actual situation, and the results of this study can only be used for
25 initial determination, which should be supplemented by further research.

26 **3.5.2 SIGMA/W analytical results**

27 SIGMA/W displacement analyzed its initial boundary condition settings, as shown in Fig. 29.
28 The boundaries AC and ED are the fixed boundaries of horizontal displacement; CD is set to
29 be the fixed boundary of vertical and horizontal displacement; AE applies building loads
30 according to the cross-sectional position of the buildings, as shown in Fig. 29. There are three
31 buildings in the cross-section profile: Hua-Fan Temple, Wu-Ming Building, and Jue-Zhao
32 Building. The loads applied are 10 kPa, 50 kPa, and 50 kPa, respectively. Table 5 shows the



1 settings of the remaining loads, and Table 6 shows the input parameters for the SIGMA/W
2 numerical model analysis.

3 Figure 30 shows the SIS-20 and SIS-11 inclinometer displacement increment diagram during
4 the typhoon Soudelor; Fig. 31, the typhoon Goni; and Fig. 32, the southern low-pressure
5 system (Aere typhoon). These figures demonstrate the displacement result simulated by this
6 model has the same displacement curve trend as the actual monitoring data. There is a slightly
7 different analytical value at the shear zone, with an alignment error value of only 0–2 mm. A
8 possible reason for the error is that simulated soil layer mesh has uneven nodes. In future
9 studies, this module can be modified to apply the continuous shear test to adjust the input
10 parameters and soil layer mesh size to change the settings. The actual displacement value
11 from the typhoon rainfall observation can be further expanded for comparative analysis, in
12 order to arrive at a more accurate prediction of the slope displacement results caused by future
13 typhoon rainfalls and to provide the campus a reference for slope safety.

14 Based on the above results, it is presumed that the reason of simulation results showing
15 difference in the present observation data is that the actual displacement amount of SAA is all
16 within 20 mm (2 cm). For cumulative rainfall and peak rainfall smaller than 60 mm, the
17 change in the output result by the simulated rainfall is extremely small, therefore leading to
18 the error. The result agrees with the results mentioned above in Table 2; generally, only when
19 the rainfall exceeds 77 mm will the displacement be driven. In other words, simulation results
20 from the software using cumulative rainfall and peak rainfall greater than 60 mm will be more
21 important and more meaningful than simulation results from simulating a single-peak rainfall.
22 Future studies should conduct the simulation in this manner.

23 **3.5.3 SLOPE/W analytical results**

24 The strata strength parameter input for the analysis of SLOPE/W was the same as the input
25 parameter value of SIGMA/W model analysis.

26 The analysis method adopted two modes:

27 (1)The minimum safety factor of sliding surface was calculated within the specified range of
28 the slope. (2) Since the current inclinometer monitoring records clearly show the sliding
29 surface depth, the sliding surface known is adopted in the numerical model for slope stability
30 analysis, and the sliding depth is connected from each inclinometer record as a reference for
31 determining the sliding range. This study adopted the Morgenstern-Price extreme balance
32 method to calculate the safety factor of the sliding surface. Figure 33 shows the profile of



1 SLOPE/W analysis. The most critical potential sliding surface existed between Jue-zhao
2 building and Wu-ming building is shown in the profile. The results of safety factor variation
3 during typhoon are shown in Fig. 34.

4 Fig. 34 shows that during the typhoons Soudelor and Goni, although the safety factor of the
5 slope will drop to about 0.4, the minimum safety factor for rainfall can still be maintained at
6 1.3. This illustrates that even though typhoon rainfall will cause a certain amount of slope
7 displacement at the campus, its safety factor is still higher than the general suggested value of
8 1.2; in other words, there is not yet immediate danger of sliding. However, further studies
9 should investigate the impact on safety factors in situations of higher typhoon rainfall through
10 actual follow-up test results and feedback analyses.

11

12 **4 CONCLUSIONS AND SUGGESTIONS**

13 This paper offers a comprehensive survey of the slope behavior during rainfall infiltration,
14 including the highest groundwater level measured within the slope, the time lag reaction of
15 groundwater variations, the influence of rainfall types and amount, the relationship curve of
16 rainfall amount and groundwater level, and a review of the effectiveness of the two catchpits.
17 The displacement curve measured by the inclinometers is used for feedback comparison, and
18 numerical analyses and simulations are performed to validate the changes in the behavior and
19 mechanisms. Based on the results, the following conclusions can be made:

20

21 1. When the peak rainfall is higher, there is less delay of groundwater level rise, and the peak
22 rainfall of post-peak rainfall is larger than that of other rain types, which makes the
23 groundwater-level variation large. Thus, observation up to 40 hours is needed for post-peak
24 rainfall type. The groundwater-level W1 is most affected by the rainfall, with a variation of 1–
25 23 m. The groundwater level variation was 0.6–5.8 m for W2, 0.25–3.1 m for W3, and 0.1–2
26 m for W4.

27 2. After the implementation of the catchpits, the lowest groundwater level has decreased from
28 –43.67 m in 2015 to –52.03 m in 2016. The highest groundwater level also dropped from
29 –22.67 m to –27.84 m. Therefore, initial observations confirmed that the normal groundwater
30 level and highest groundwater level has been significantly decreased during the rainy seasons
31 and typhoon seasons by the draining effectiveness of the two catchpits.



1 3. The cumulative rainfall amount and SAA displacement increment both exhibit a certain
2 variation trend, and obtained average formula and the data in Table 2 can be used as a
3 reference for ordinary heavy rainfall. In a typical typhoon situation, the average formula can
4 be used to deduce displacement increment, as shown in Table 3, for future reference.

5 4. When the typhoon cumulative rainfall reaches 184 mm, significant displacement will occur;
6 when the cumulative rainfall reaches 300 mm or more, or when the peak hourly rainfall
7 exceeds 100 mm, the displacement will begin to accelerate, producing displacement of larger
8 than 3 mm. Therefore, the study sets typhoon rainfall of more than 300 mm as the alert
9 threshold. If the weather forecast reports a typhoon rainfall of more than 300 mm, then
10 the displacement situation should be closely monitored.

11 5. The Geostudio groundwater-level simulation results show that the groundwater level will
12 increase during typhoons. The groundwater level variation was 0.6–1.65 m during the
13 typhoon Soudelor, 0.09–1.16 m during the typhoon Goni, and 0.01–5 m during the southern
14 low-pressure system (typhoon Aere). However, the degree of groundwater-level variations
15 was smaller than the actual monitoring data (average is 18 m), possibly due to differences in
16 the hydraulic conductivity of the simulated soil, infiltration reduction coefficient, element
17 mesh size, boundary conditions of cross-sectional variations, and parameter settings. Further
18 studies are necessary for refined model correction.

19 6. The typhoon Soudelor simulation shows that the displacement result simulated by this
20 model has the same displacement curve trend as the actual monitoring data. There is a slightly
21 different analytical value at the shear zone, with an alignment error value of only 0–2 mm. A
22 possible reason for the error is that simulated soil layer mesh has uneven nodes. In future
23 studies, this model can be modified to apply the continuous shear test and adjust the soil layer
24 mesh size to change the settings. The actual displacement value from typhoon rainfall
25 observation can be further expanded for comparative analysis, in order to reach a more
26 accurate prediction of slope displacement caused by future typhoon rainfalls and to provide
27 the campus a reference for slope safety.

28 7. The displacement amount SAA is all within 20 mm. For cumulative rainfall and peak
29 rainfall smaller than 60 mm, the change in the output result by the simulated rainfall is
30 extremely small, therefore leading to the error. The result agrees with the results mentioned
31 above; generally, only when the rainfall exceeds 77 mm will the displacement be driven. In
32 other words, simulation results from the software using cumulative rainfall and peak rainfall



1 greater than 60 mm will be more important and more meaningful than simulation results from
2 simulating a single peak rainfall. Future studies should conduct the simulation in this manner.
3 8. The slope model analytical results show that during the typhoons Soudelor and Goni,
4 although the safety factor of the slope will drop to 0.4, the minimum safety factor for rainfall
5 was still maintained at 1.3, higher than the general suggested value of 1.2. This means that
6 there is not yet any immediate danger of sliding. However, future studies should follow up
7 with the actual test results and feedback analysis to reach a more comprehensive
8 understanding of the impact of rainfall on the safety factors in situations of higher typhoon
9 rainfall.

10

11 **Author Disclosure Statement**

12 No competing financial interests exist.

13

14 **Acknowledgements**

15 This study is funded by the Ministry of Science in Taiwan as under project number MOST
16 105-2632-M-211-001. The authors are grateful for the support, which made it possible for the
17 study to proceed and conclude smoothly.

18

19 **References**

20 Chao, C. P.: The GIS structure of disaster prevention for Ta-Lun Shan area and application
21 Case, Proceedings of the Symposium on Slope Land Disaster and Prevention, 2002.

22 Chao, C. P.: The study of the establishment of creep model by using the monitoring data of
23 slope land, Journal of the Chinese Institute of Civil and Hydraulic Engineering, 15, (3), 467–
24 476, 2003.

25 Huang, C. S. and Jeng, C. J.: A supplementary geological survey and analysis of the Talun
26 area around the Huafan University. Journal of Art and Design of Huafan University, (1), 59–
27 69, 2004.

28 Japan Landslide Association for Slope Disaster Management (JASDiM): Essential
29 implementation of technical design for landslide countermeasures, (2), 22, 1978 (in Japanese).



- 1 Jeng, C. J.: Study on slope stability mechanism of Huafan University by using of inclinometer
2 displacement and limiting equilibrium stability analysis. *Journal of Huafan University*, (9),
3 115–127, 2003.
- 4 Jeng, C. J., Chu, B. L., Tsao, S. P., and Lin, T. A.: Matrix suction of unsaturated colluvium
5 slope influenced by rainfall and plant condition: A case of Taiwan Huafan University. *Wuhan*
6 *University Journal of Natural Sciences*, 12, (4), 689–694, 2007.
- 7 Jeng, C. J., Sue, D. Z., and Chen, P. J.: A case study of the buildings inclination observation
8 and ground movement monitoring for the school on the slope. *Proceeding of Conference on*
9 *Design and Cultural of Huafan University*, 2009.
- 10 Jeng C. J., and Lin, T. A.: A case study on the in-situ matrix suction monitoring and
11 undisturbed-sample laboratory test for the unsaturated colluvium slope. *Soils and*
12 *Foundations*, 51, (2), 321–331, 2011.
- 13 Jeng, C. J. and Jiang, J. R.: Research on serial behaviors of colluviums slope from rainfall
14 infiltration caused ground water variation to the slope stability and displacements. *Journal of*
15 *Art and Design of Huafan University*, (8), 17–31, 2013.
- 16 Jeng, C. J. and Lin, C. H.: Relationship between slope displacement and rainfall and setting of
17 warning value. *Proceedings of Cross-Strait Conference on Soil and Water Conservation*,
18 *Wuhan, Hubei, China*, 416–427, 2014.
- 19 Jeng, C. J. and Yang, C. Y.: A case study on groundwater variation and slop displacement
20 induced by rainfall. *Journal of Art and Design of Huafan University*, (10), 141–156, 2015.
- 21 Jeng, C. J., Tsao, S. P., Lee, Z. J., Chen, S., Chen, K. Y., and Yang, C. Y.: Integration
22 research on the rainfall threshold value setting for the deformation triggering by typhoon and
23 disaster prevention response system. *Proceedings of Cross-Strait Conference on Soil and*
24 *Water Conservation*, 310–331, 2015.
- 25 Jeng, C. J. and Sue, D. Z.: Characteristics of ground motion and threshold values for
26 colluvium slope displacement induced by heavy rainfall. *Nat. Hazards Earth Syst. Sci.*, (16),
27 1309–1321, 2016.
- 28 Xu Q.: Early warning and emergency disposal of landslide disaster, state key laboratory of
29 geohazard prevention and geoenvironment protection: An academic report in National Chung
30 Hsing University, Taiwan, 2011.



1

2 Table 1: Typhoon cumulative rainfall alert threshold values for each inclinometer

Inclinometer number	Threshold (mm)
SIS-1	420
SIS-5	420
SIS-7	350
SIS-17	420
SIS-20B	370
SIS-25A	420
SIS-32	350
SIS-33B	315
SIS-40	460

3

4 Table 2: Daily cumulative rainfall from heavy rainfall days and SAA displacement increment

Term	Daily cumulative rainfall (mm / day)	SAA displacement increment (mm)
1	77–150	0.21–0.34
2	150–300	0.34–1.03
3	300–500	1.03–1.95
4	> 500	1.95

5

6

7

8



1 Table 3: Daily cumulative rainfall and SAA displacement increment for general typhoon
 2 conditions.

Term	Daily cumulative rainfall (mm / day)	SAA displacement increment (mm)
1	68.5–150	0.42–0.56
2	150–300	0.56–0.80
3	300–500	0.80–4.17
4	> 500	> 4.17

3

4 Table 4: Input parameters

Soil layer	Seepage mode	k (cm / s)
Colluviums layer	Saturation	10^{-3}
Sandstone and shale interbedded	Saturation	10^{-4}
Sandstone layer	Saturation	10^{-5}
Shear zone	Saturation	$1.39 \cdot 10^{-5}$

5

6 Table 5: Building load parameters

Building name	Applied load (kPa)
Hua-fan temple	10
Wu-ming building	50
Chea-chau building	50

7



1 Table 6: Input Parameters for numerical analysis

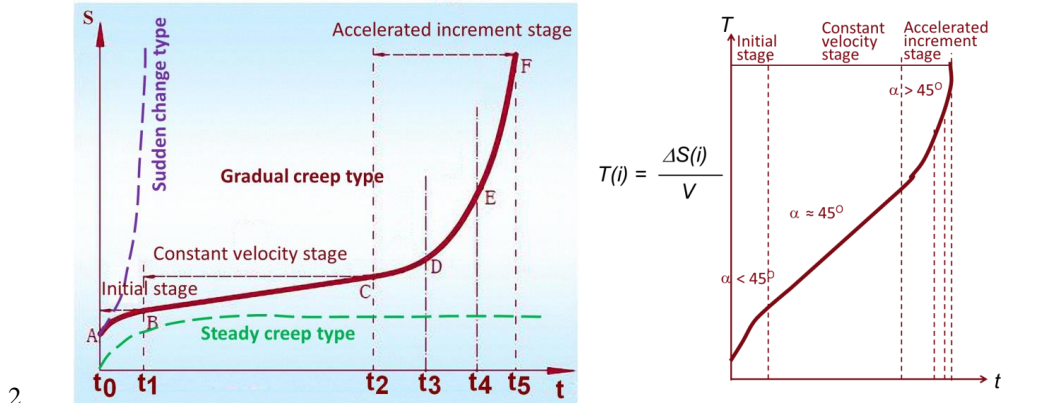
Soil layer	Colluvium soil layer	Sandstone and shale interbedded	Gravel layer	Shear zone
Deformation model	Elastoplastic	Elastoplastic	Linear elasticity	Interface elements
Elastic modulus (kPa)	3×10^4	3.225×10^5	3.753×10^6	3748
Poisson's ratio	0.334	0.28	0.23	0.334
Unit weight (kN/ m ²)	19.31	25.52	23.86	23.3
Cohesion, C (kN/ m ²)	18.5	41.8	38.7	0
Internal friction angle, Φ (degrees)	29.6	32.13	32.74	23

2

3



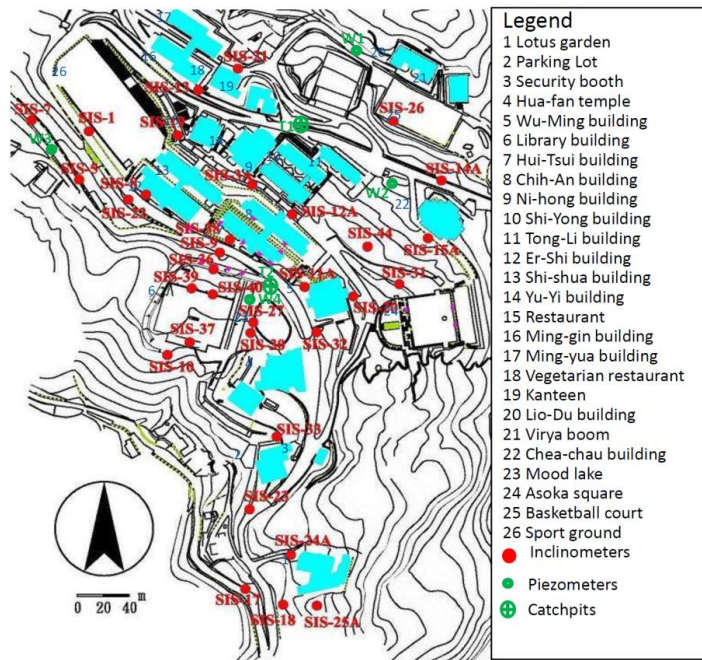
1 **Figures and captions**



2
 3
 4
 5
 6

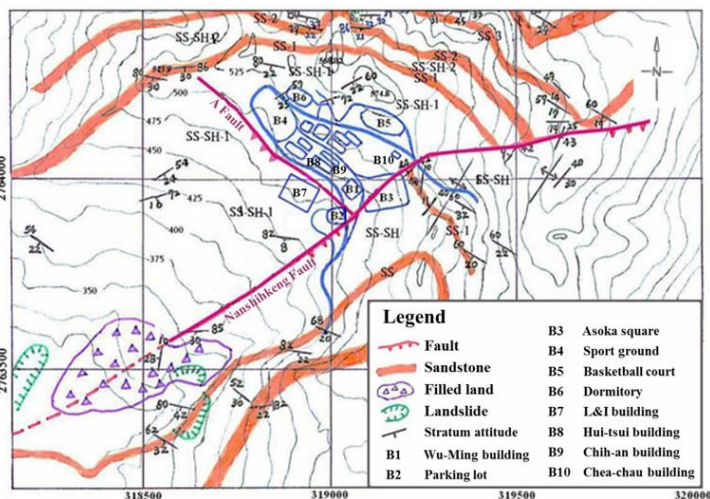
Figure 1: S-t curve of slope sliding displacement (a) and T-t curve of slope sliding displacement (b) (modified after Xu et al., 2008 and Xu, 2011).

6



7

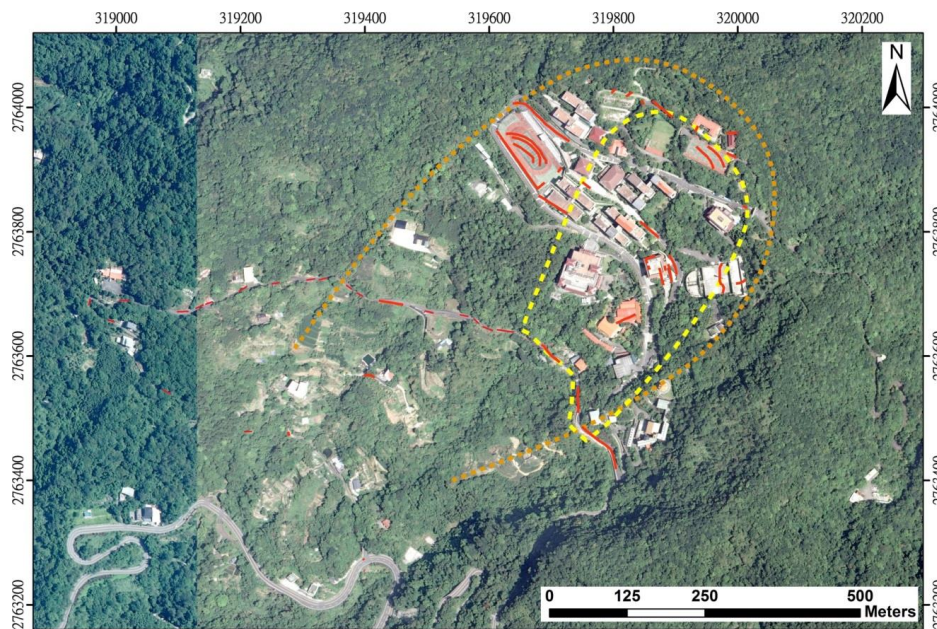
8 Figure 2: Inclinometer distribution at the Huafan campus



1

2 Figure 3: Geological map of the research area (Huang and Jeng, 2004)

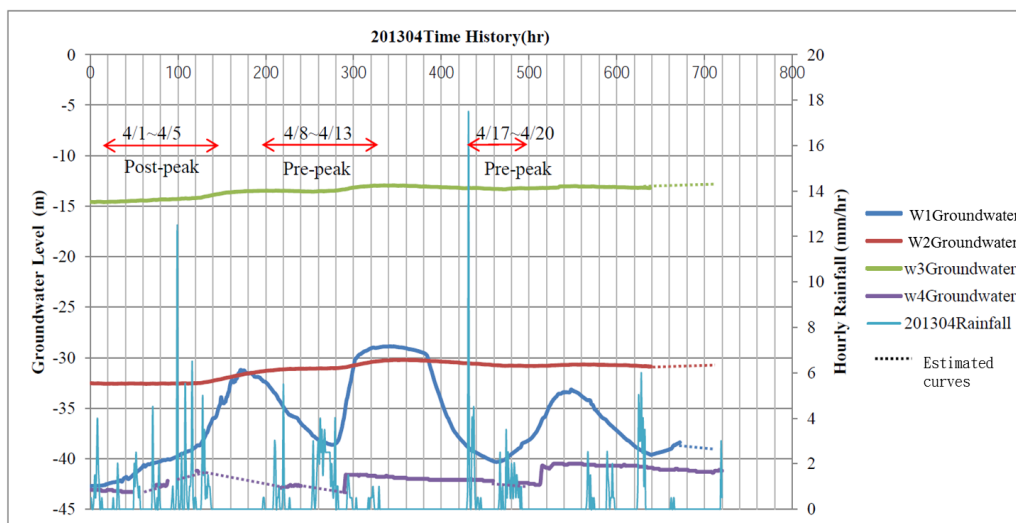
3



4 Sliding area M1 Sliding area R1 Tension crack

5 Figure 4: Location of surface cracks inside and outside the campus.

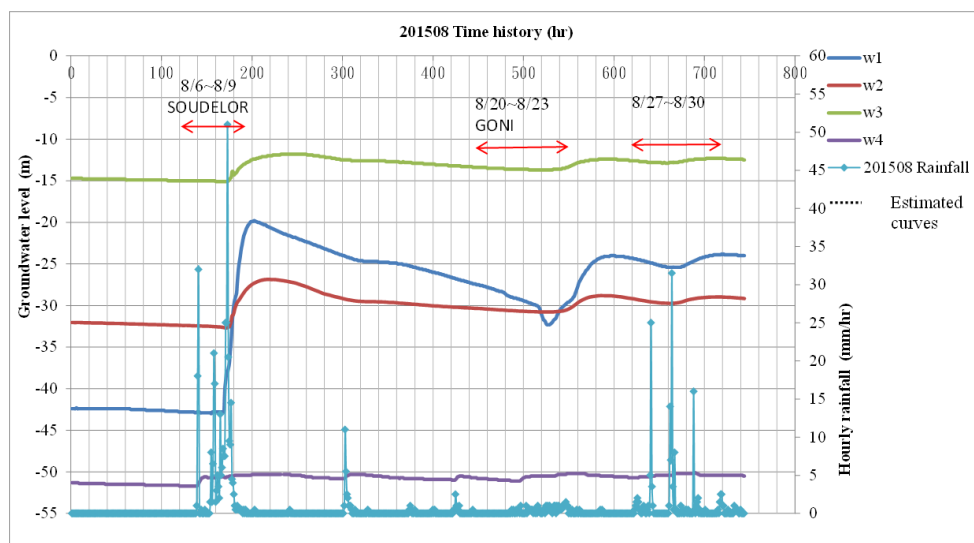
6



1

2 Figure 5: Groundwater level and rainfall duration curves from auto-recording groundwater-
 3 level gauge in April 2013.

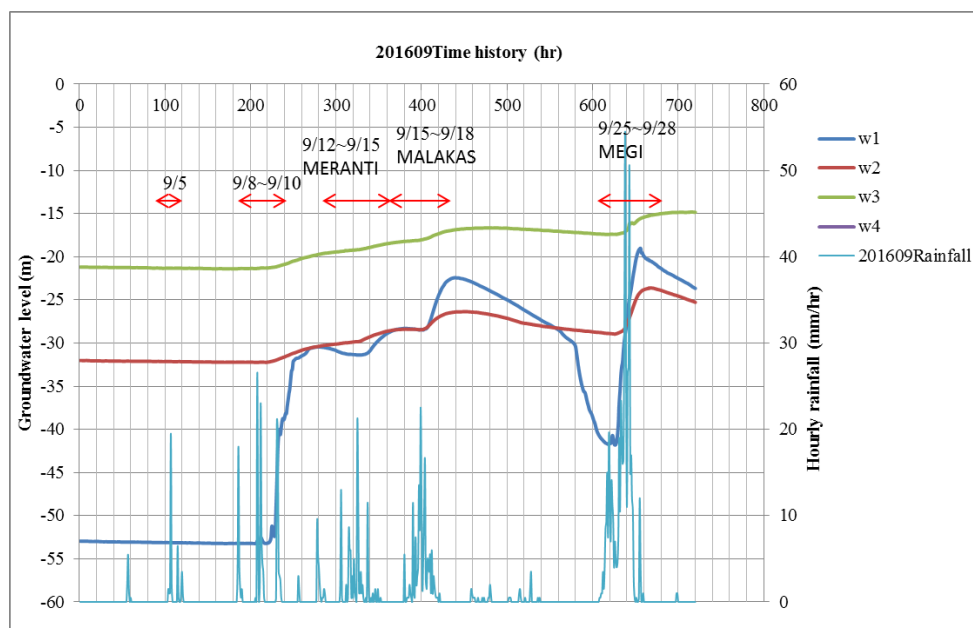
4



5

6 Figure 6: Groundwater level and rainfall duration curves from auto-recording groundwater-
 7 level gauge in August 2015.

8

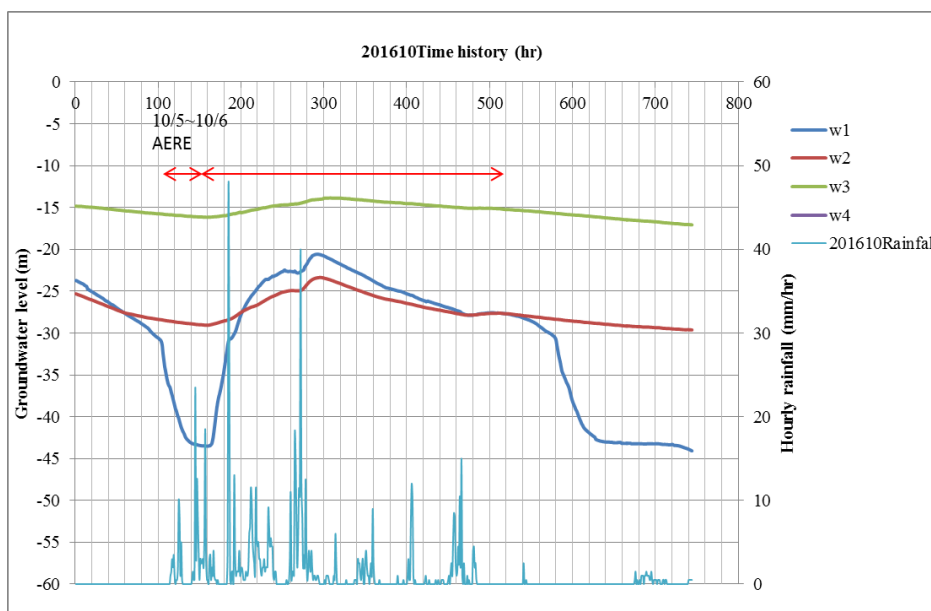


1

2 Figure 7: Groundwater level and rainfall duration curves from auto-recording groundwater-
3 level gauge in September 2016.

4

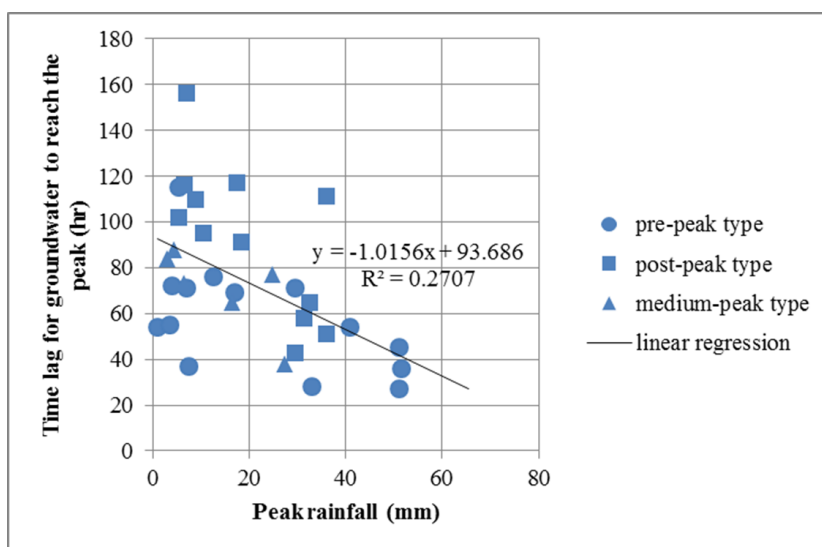
5



1

2 Figure 8: Groundwater level and rainfall duration curves from auto-recording groundwater-
 3 level gauge in October 2016.

4

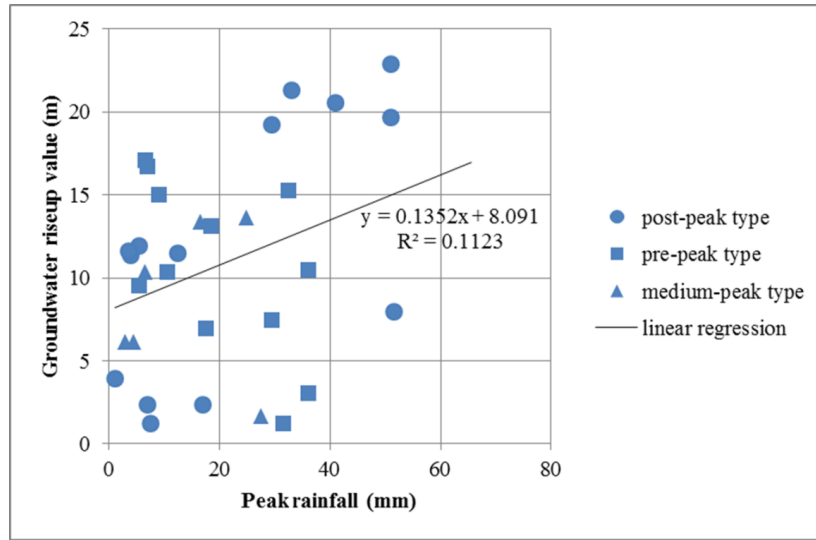


5

6 Figure 9: Groundwater level and time lag of rainfall peak diagram of automatic groundwater-
 7 level gauge W1.



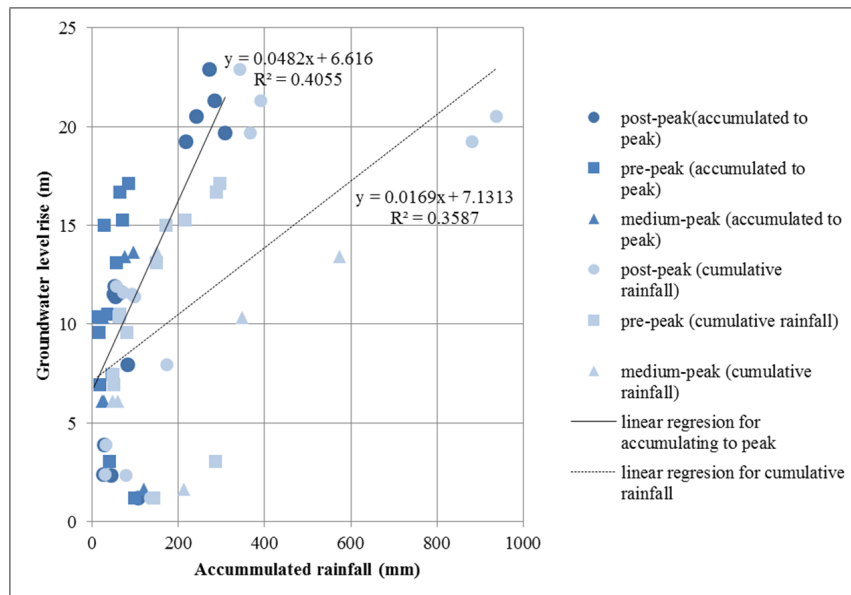
1



2

3 Figure 10: Peak rainfall and groundwater level rise diagram of automatic groundwater-level
 4 gauge W1.

5



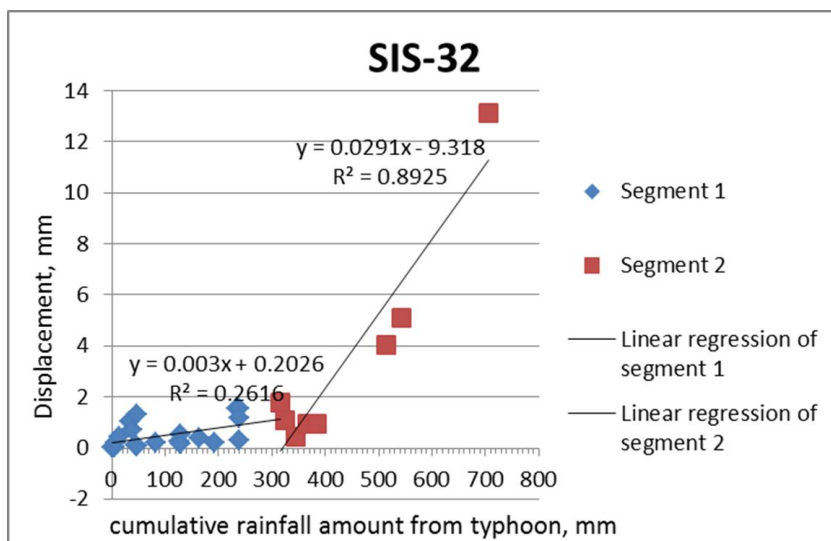
6

7 Figure 11: Accumulated rainfall and groundwater level rise diagram of automatic



1 groundwater-level gauge W1.

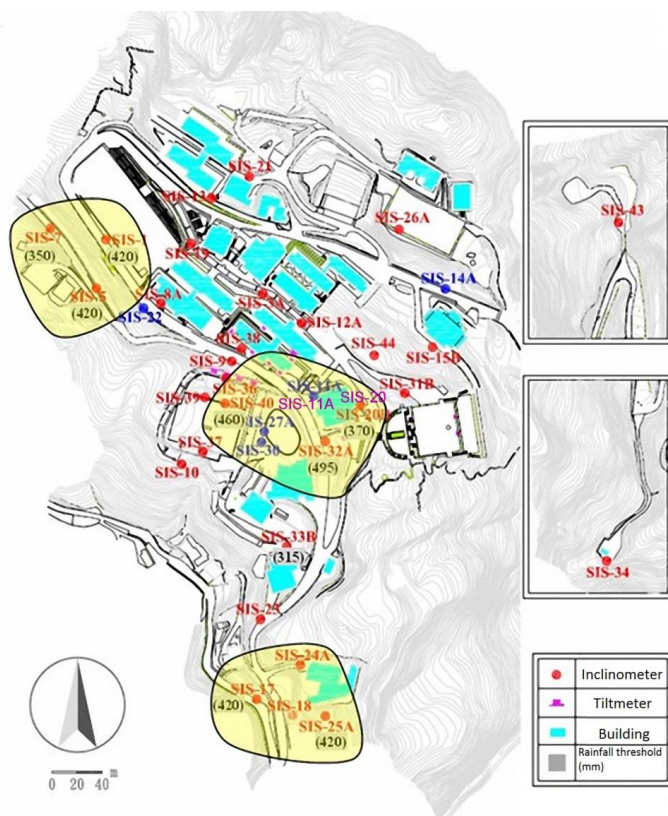
2



3

4 Figure 12: SIS-32 displacement and cumulative rainfall amount from typhoon rainfall.

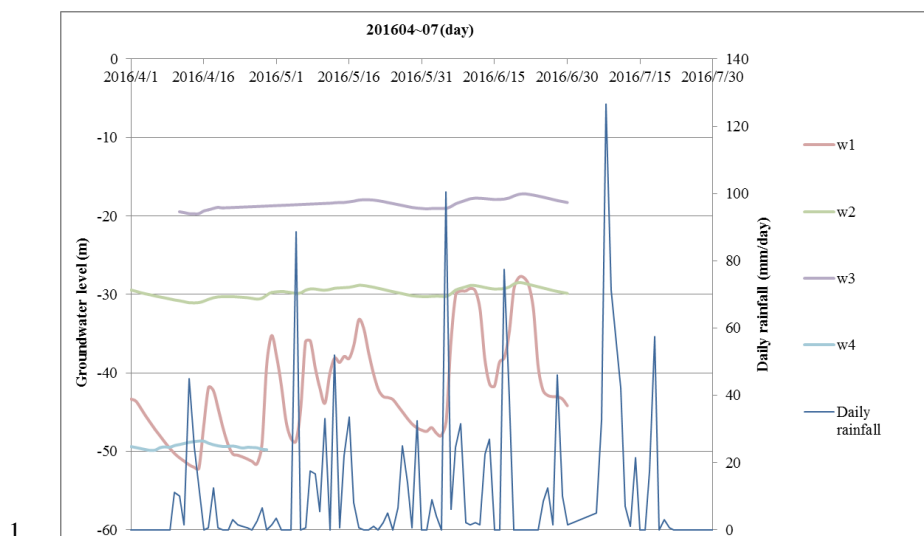
5



1

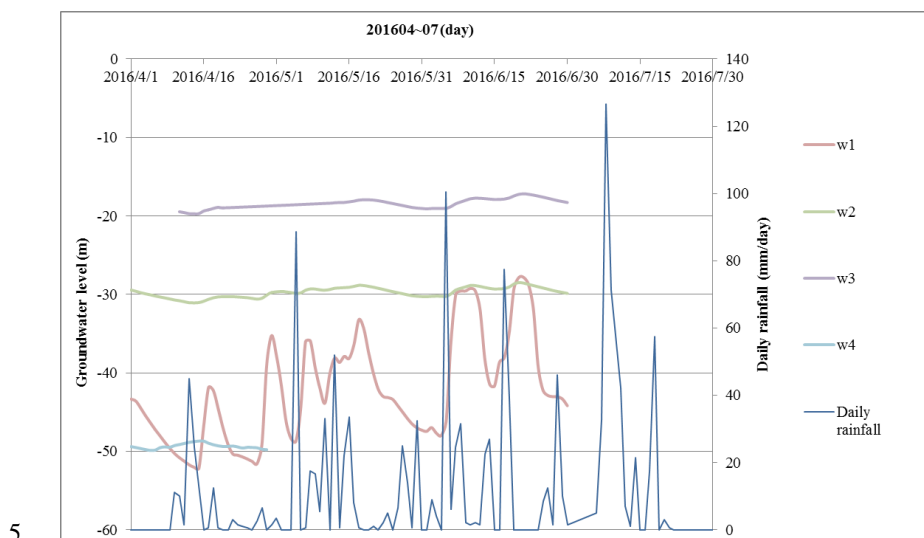
2 Figure 13: Positions of the inclinometers where alert rainfall threshold has been reached
3 during typhoon rainfalls.

4



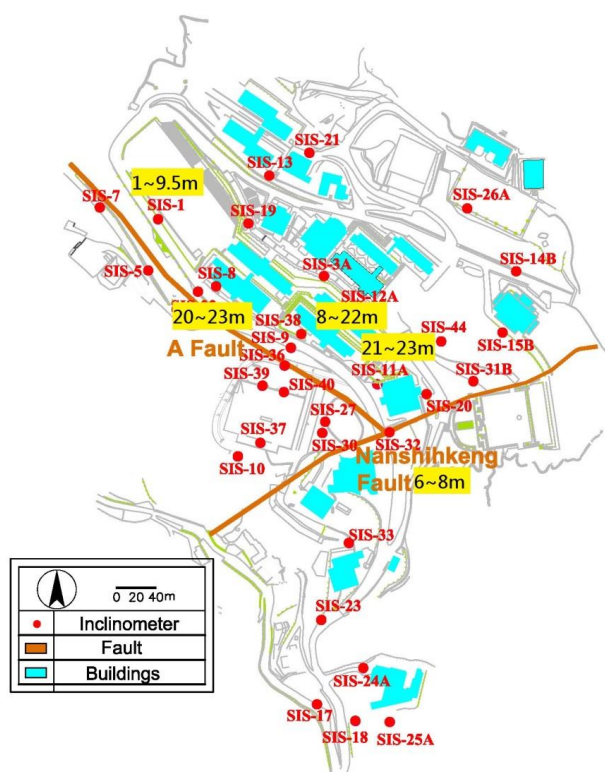
2 Figure 14: Time graph of groundwater level and rainfall amount from auto-recording
3 groundwater-level gauge from April to July 2016.

4



6 Figure 15: Comparison of groundwater level before and after catchpits implementation.

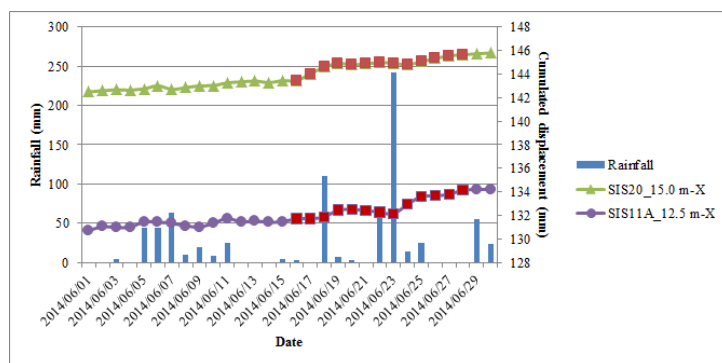
7



1

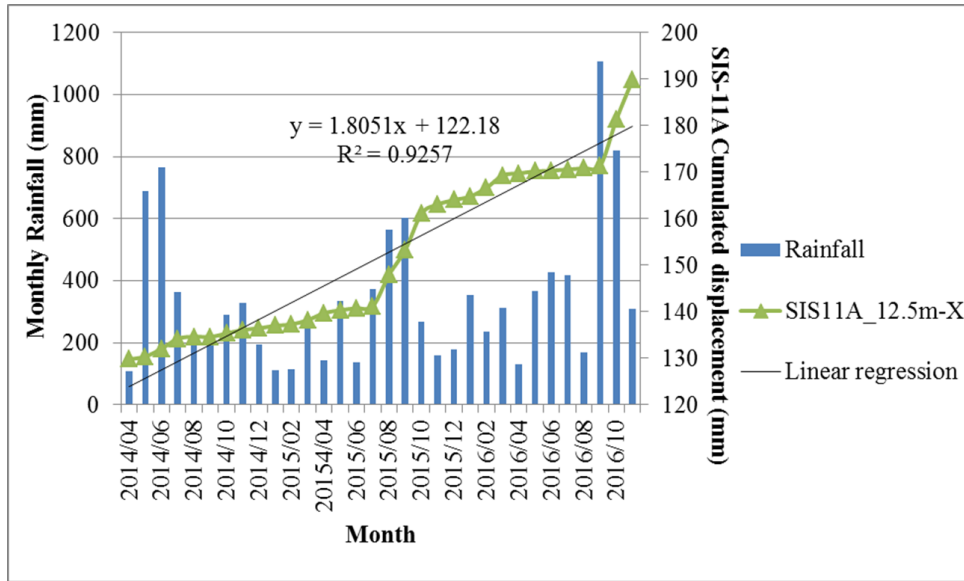
2 Figure 16: Groundwater level rise amount distribution from highest groundwater-level gauges
 3 and SAA locations.

4



5

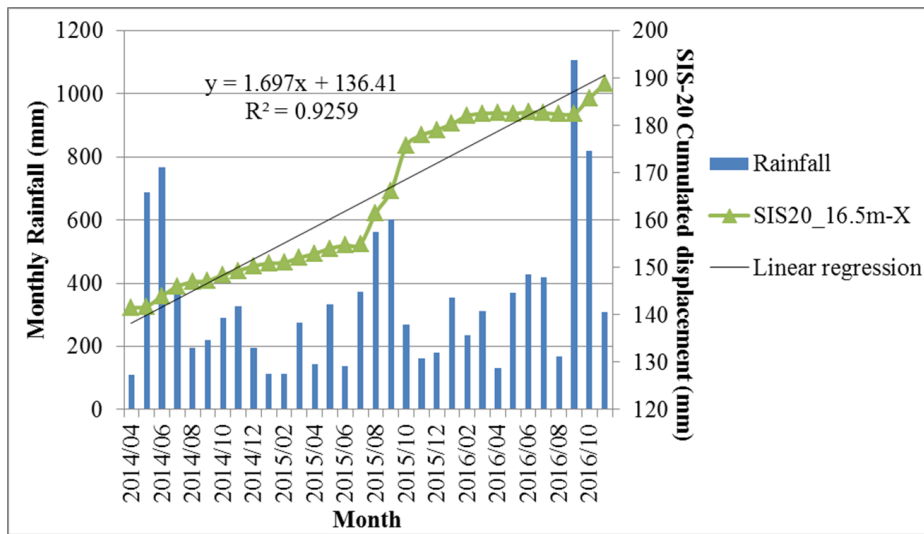
6 Figure 17: Relationship between SIS-11 and SIS-20 displacement and rainfall amount from
 7 June 2014.



1

2 Figure 18: SIS-11 displacement versus rainfall amount (as in February 2017).

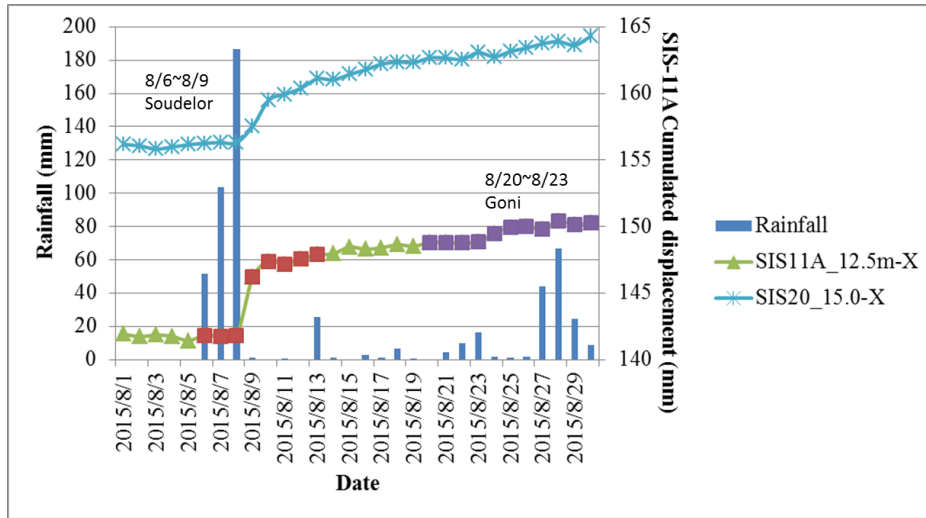
3



4

5 Figure 19: SIS-20 displacement versus rainfall amount (as in February 2017).

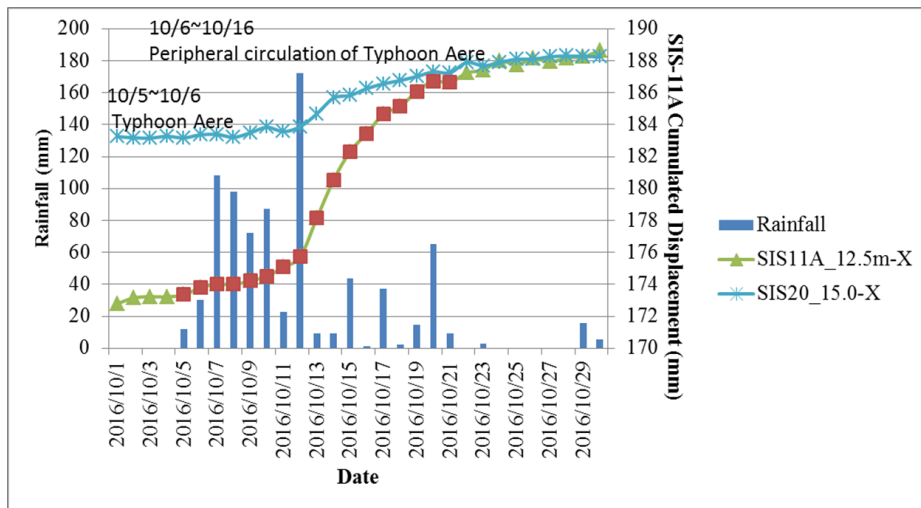
6



1

2 Figure 20: SIS-11 and SIS-20 displacement versus rainfall amount in August 2015.

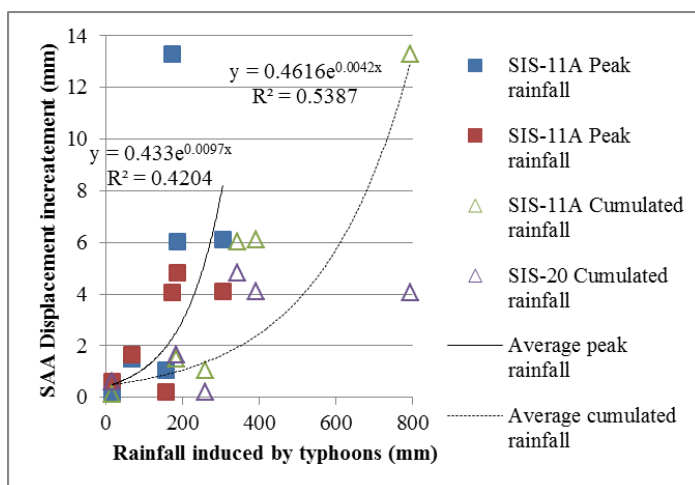
3



4

5 Figure 21: SIS-11 and SIS-20 displacement versus rainfall amount in October 2016.

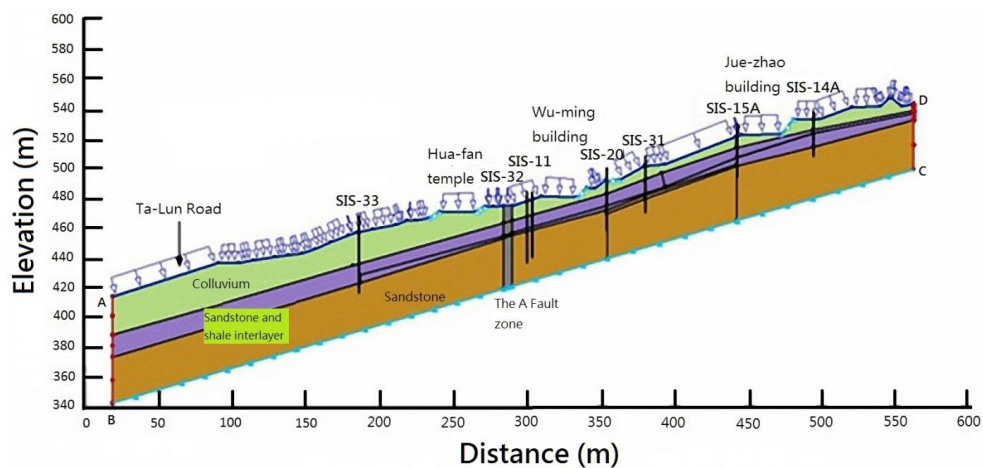
6



1

2 Figure 22: SAA displacement increment during typhoon rainfall.

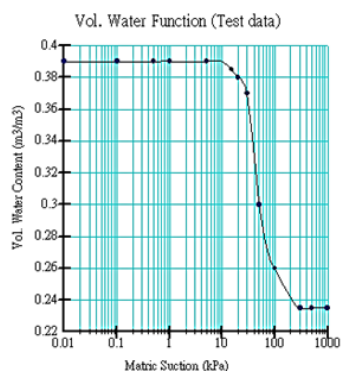
3



4

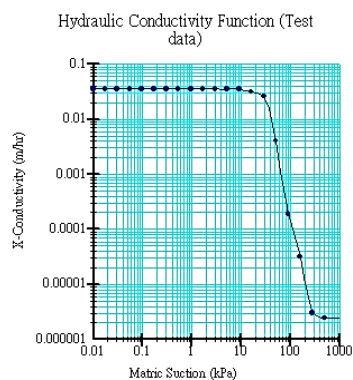
5 Figure 23: Cross-section profile of SEEP/W.

6



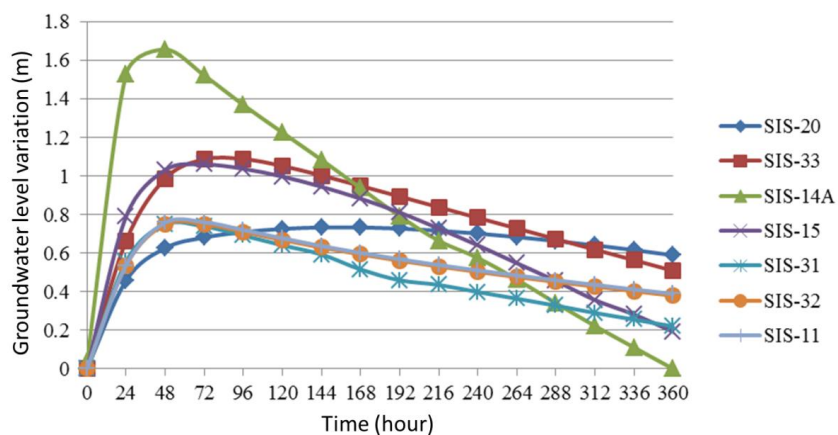
1
2 Figure 24: Soil water characteristic curve.

3



4
5 Figure 25: Hydraulic conductivity curve.

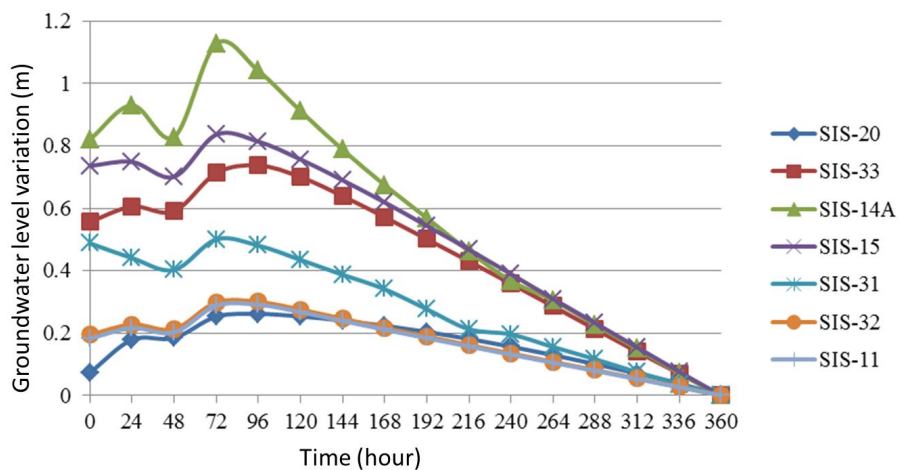
6



1

2 Figure 26: Simulation of groundwater-level variation during the typhoon Soudelor.

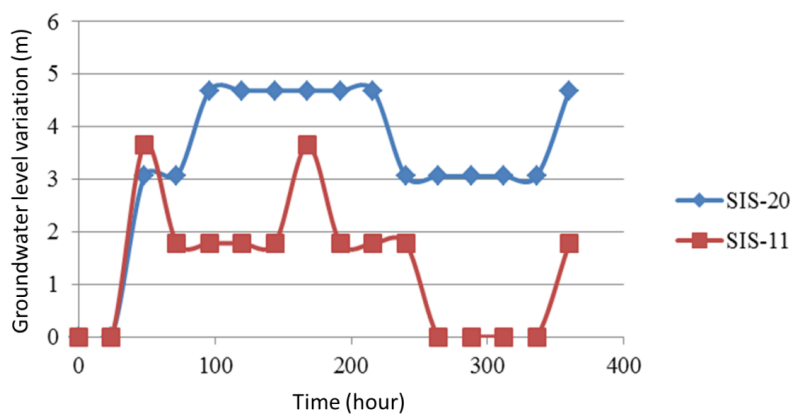
3



4

5 Figure 27: Simulation of groundwater-level variation during the typhoon Goni.

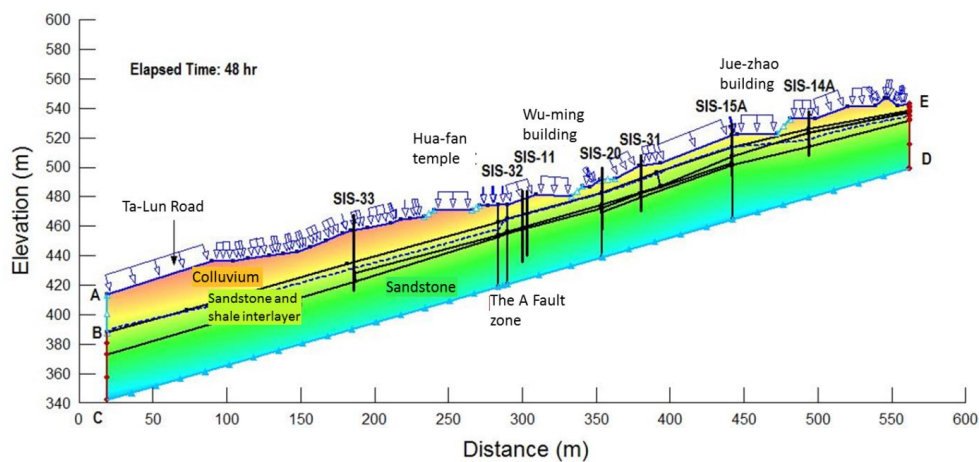
6



1

2 Figure 28: Simulation of groundwater-level variation for the southern low-pressure system
 3 (Aere typhoon)

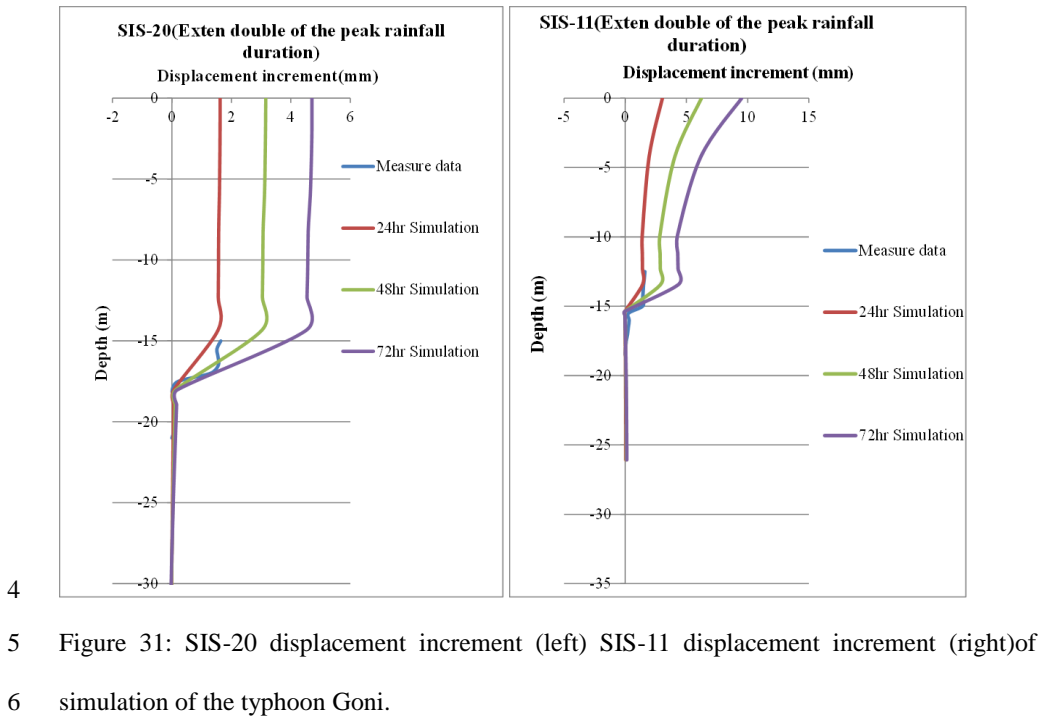
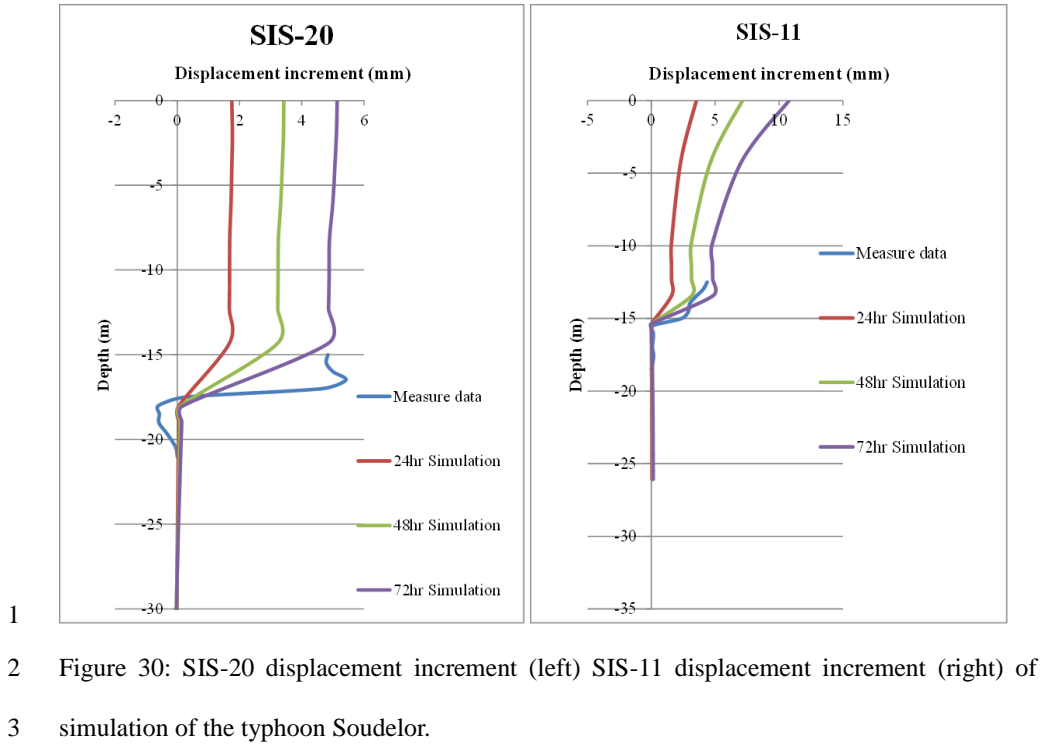
4

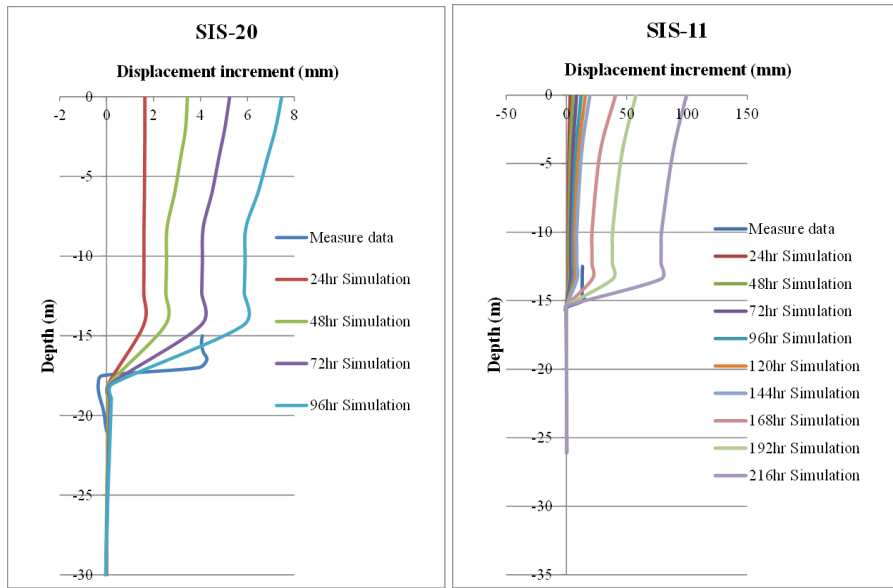


5

6 Figure 29: Cross-sectional view of SIGMA/W.

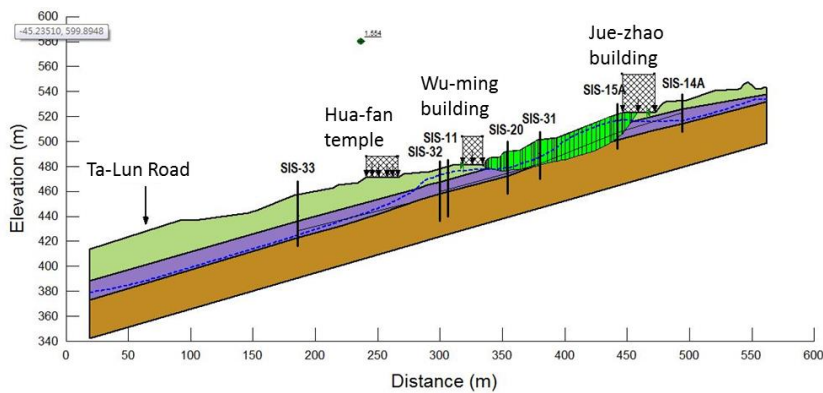
7





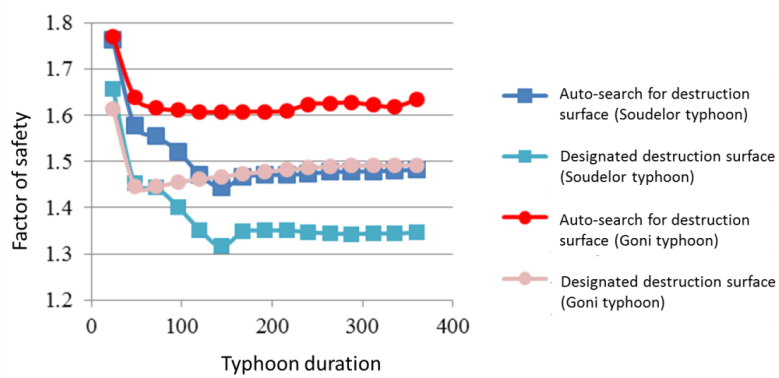
1
 2 Figure 32: SIS-20 displacement increment (left) SIS-11 displacement increment (right) of
 3 simulation of the southern low-pressure system (typhoon Aere).

4



5
 6 Figure 33: Profile of potential sliding surface analysis

7



1

2 Figure 34: Variation of safety factor in typhoon simulation.